FRET imaging of *Teen* sensor captures ERK activation changes preceding morphological defects in a RASopathy zebrafish model and phenotypic rescue by MEK inhibitor

Fasano *et al.*,

SUPPLEMENTARY MATERIAL

Supplementary Figure 1: *In vivo* time lapse in *Teen* embryos obtained by spectral unmixing-FRET protocol reporting high ERK activity in zebrafish embryos from late gastrulation till segmentation stage.

Supplementary Figure 2: Live reporting of increased ERK activity captured in zebrafish embryos at circa 15-16 hpf expressing the FRET-based ERK sensor *Teen* upon acute EGF treatment.

Supplementary Figure 3: Increased pERK/tERK signal upon acute treatment of 24 hpf wild-type embryos with EGF is validated by immunofluorescence and western blot analysis.

Supplementary Figure 4: Supplementary Figure 4: Decreased pERK signal upon chronic exposure to SHP099 is validated by western blot analysis and increased R_{DA} values calculated from AB-FRET data of *Teen* embryos treated with SHP099.

Supplementary Figure 5: Visual correlation between AB-FRET efficiency and derived R_{DA} values obtained by AB-FRET in 5-6 hpf zebrafish *Teen* embryos over-expressing WT and mutant (D61G) Shp2.

Supplementary Figure 6: Decreased ERK signal in NS embryos (expressing $Shp2^{D61G}$) treated with low-dose MEK inhibitor as measured by spectral unmixing-FRET during late gastrulae, bud and segmentation stages (9, 10 and 11-12 hpf).

Supplementary Figure 7: Embryo shortening in NS models is rescued by low-dose PD treatment (0.25 μM) but worsened by high doses (1 μM).

Supplementary Movie 1: *In vivo* time lapse movie obtained by spectral unmixing-FRET module (xyλzt) reporting ERK activity map of a zebrafish control *Teen* embryo from late gastrulation (~ 9 hpf) till late segmentation stage (~ 18 hpf) with a time interval of 30 min.

Supplementary Movie 2: *In vivo* time lapse movie obtained by xyzt scanning of CFP and YFP (FRET) signal from a *Teen* embryo before and after EGF bath stimulation with a time interval of 10 min.

Source data

Source data containing raw uncropped blots and raw data relative to main/supplementary figures.

FRET imaging of *Teen* sensor captures ERK activation changes preceding morphological defects in a RASopathy zebrafish model and phenotypic rescue by MEK inhibitor

Fasano *et al.*,

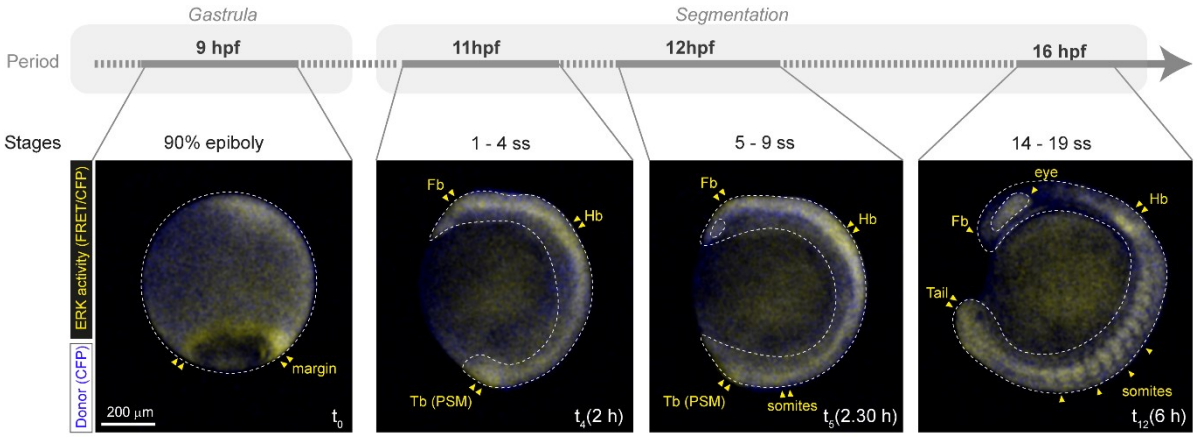

Supplementary Figure 1: *In vivo* time lapse in *Teen* embryos obtained by spectral unmixing-FRET protocol reporting high ERK activity in zebrafish embryos from late gastrulation till segmentation stage. Schematics depicts zebrafish early developmental stages from late gastrulation to somitogenesis in which pERK signal increase (FRET/CFP ratiometric image in yellow, indicated by arrows) was recorded using spectral unmixing FRET protocol in *Teen* embryos. Regions with high ERK activity are initially limited to gastrula margin (~ 9 hpf), are observed in the tailbud/presomitic mesoderm (Tb PSM), forebrain (Fb) and hindbrain (Hb) (~ 11 hpf) as well as in early born (~ 12 hpf) and mature somites (~ 16 hpf). A dashed white line outlines the developing embryo. Donor (CFP) is shown in blue.

FRET imaging of *Teen* sensor captures ERK activation changes preceding morphological defects in a RASopathy zebrafish model and phenotypic rescue by MEK inhibitor

Fasano *et al.*,

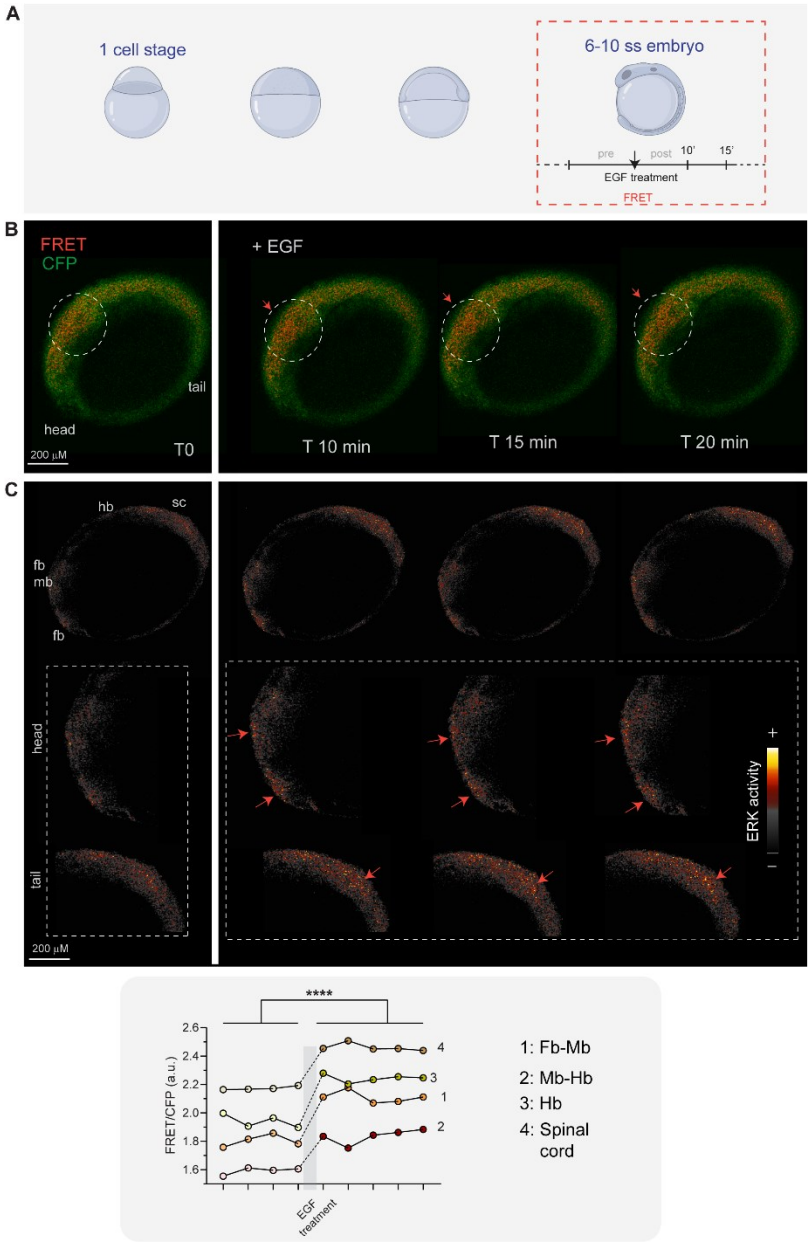

Supplementary Figure 2: Live reporting of increased ERK activity captured in a zebrafish embryo at segmentation stage expressing the FRET-based ERK sensor *Teen* upon acute EGF treatment. (**A**) Schematics depicting zebrafish early development and circa 10 ss stage (red square) in which acute (10') treatment with rat EGF and FRET imaging was perfomed. FRET data were captured using donor excitation and collection of donor and acceptor emission spectra for a defined nm range (ratiometric module). (**B**) Sum-intensity projection of confocal *x,y,z* live scans of a single embryo showing FRET (YFP, red) and CFP (donor, green) signal before (T0) and at three different time points after EGF treatment. Representative pERK signal increase (FRET channel) in the hindbrain region well visible by the embryo orientation is indicated by a dashed white circle. (**C**) Single superficial z-layer for the FRET channel at different time points rendered with the "smart" LUT intensity scale in Fiji. Fb, Mb, Hb: forebrain, midbrain, hindbrain, respectively. The middle and lower panels show magnification on "head" and "tail" regions, respectively, marked by a white dashed line. Areas of clear signal increase are indicated by red arrows. (**D**)

FRET imaging of *Teen* sensor captures ERK activation changes preceding morphological defects in a RASopathy zebrafish model and phenotypic rescue by MEK inhibitor

Fasano *et al.*,

The graph shows the quantification (a.u. = arbitrary units) and statistical support of the dynamic FRET/CFP intensity signal over time in different regions of the developing nervous system. One-way Anova is used to assess statistical significance.

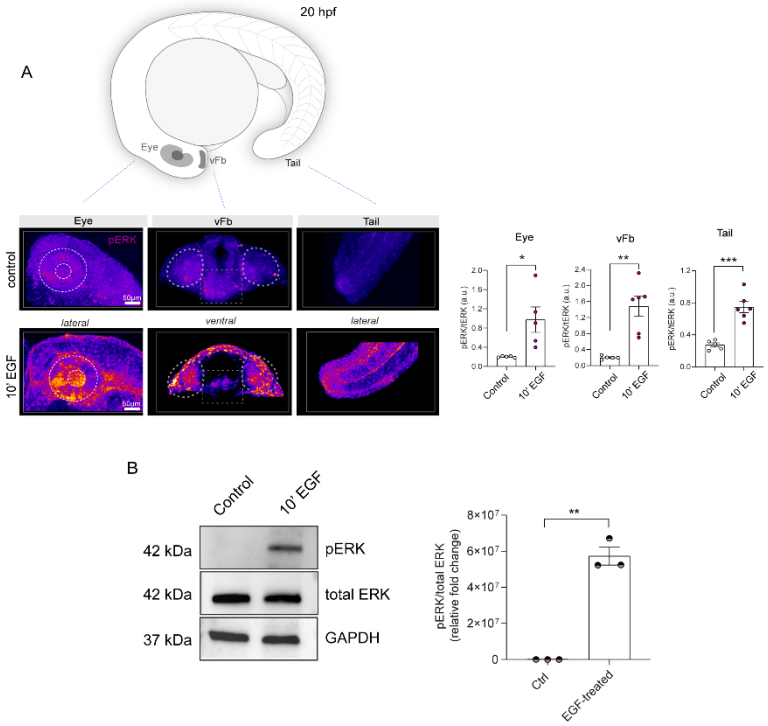

Supplementary Figure 3: **Increased pERK/tERK signal upon acute treatment of 24 hpf wild-type embryos with EGF is validated by immunofluorescence and western blot analysis.** (**A**) Immunofluorescence against phosphorylated ERK (pERK, magenta and "fire" LUT) and total ERK (tERK, green) in 24 hpf treated with DMSO vehicle control (control) or with 10' rat EGF by bath immersion. Increased signal in different regions is shown upon acute EGF treatment. VFb: ventral forebrain. Bar graph showing quantification of pERK normalized by tERK in whole embryo is reported on the upper right panel (pink square), and bar graphs showing quantification for specific regions are shown in the bottom right panel. Data are expressed as mean ± SEM, n of embryos = 5. (**B**) Western blot detection of pERK from whole embryo extracts after the same acute treatment shown in A. The bar graph shows the densitometric analysis of the pERK band. pERK signal is normalized by the intensity of tERK relative to the levels of the loading control marker GAPDH. Informative molecular weight (kDa) are reported from three independent experiments. Data are expressed as relative fold change to the loading control (mean ± SEM). In A and B, one-tailed Student's t test is used to assess the statistical significance (** $p < 0.01$).

FRET imaging of *Teen* sensor captures ERK activation changes preceding morphological defects in a RASopathy zebrafish model and phenotypic rescue by MEK inhibitor

Fasano *et al.*,

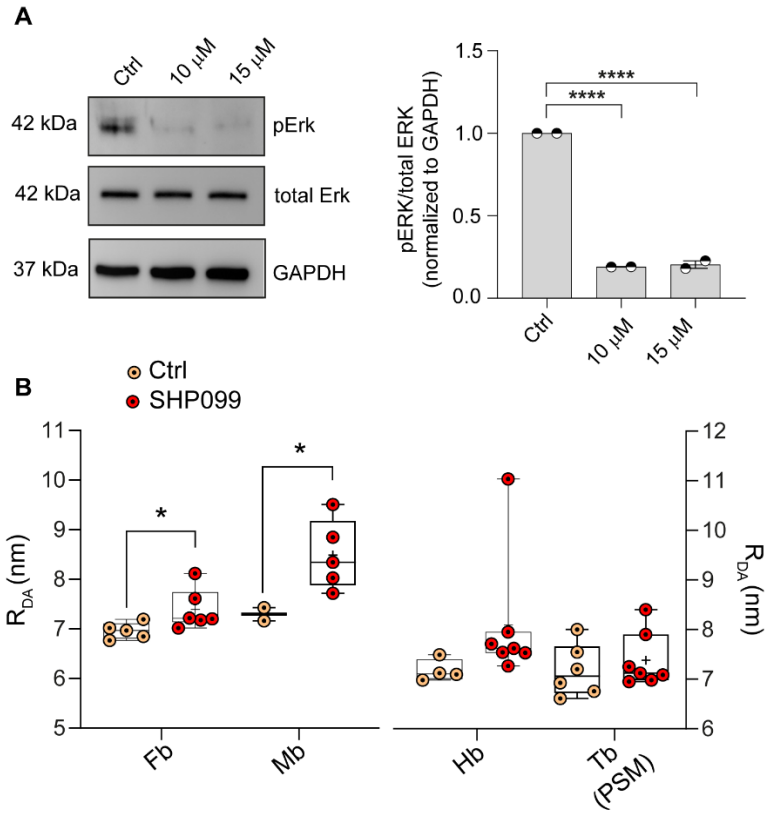

Supplementary Figure 4: Decreased pERK signal upon chronic exposure to SHP099 is validated by western blot analysis and increased R_{DA} values calculated from AB-FRET data of *Teen* embryos treated with SHP099. (A) Western blot detection of pERK from 24 hpf whole embryo extracts after chronic treatment with vehicle control or SHP099 at two different concentrations. The bar graph shows the densitometric analysis of the pERK band. pERK signal is normalized by the intensity of tERK relative to the levels of the loading control marker GAPDH. Informative molecular weight (kDa) are reported from two independent experiments. Data are expressed as relative fold change to the control (mean ± SEM). One-tailed Student's t test is used to assess the statistical significance. (**B**) R_{DA} values calculated from E data of 24 hpf zebrafish expressing the FRET-based ERK sensor Teen upon prolonged SHP099 treatment. The box plot with median (middle line), 25th–75th percentiles (box), and min–max values (whiskers) shows the R_{DA} quantification (nm) in different regions. Fb: forebrain (n = 4 and 5 for control and treated), Mb: midbrain (n = 2 and 5 for control and treated), Hb: hindbrain (n = 4 and 7 for control and treated), Tb, PSM tail bud, PSM: presomitic mesoderm (n = 6 and 7 for control and treated). One-tailed Student's t test is used to assess statistical significance (* $p < 0.05$).

FRET imaging of *Teen* sensor captures ERK activation changes preceding morphological defects in a RASopathy zebrafish model and phenotypic rescue by MEK inhibitor

Fasano *et al.*,

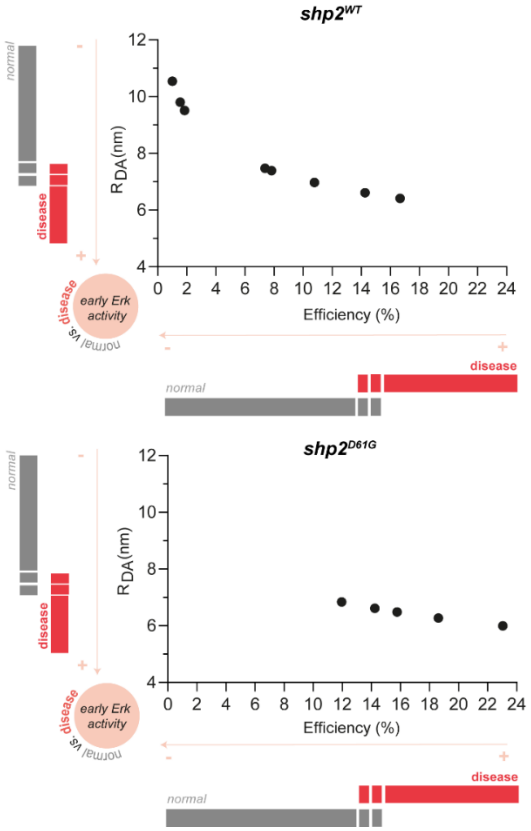

Supplementary Figure 5. Visual correlation between AB-FRET efficiency and derived R_{DA} values obtained by AB-FRET in 5-6 hpf zebrafish *Teen* embryos over-expressing WT and mutant (D61G) Shp2. Graphs show the RDA quantification (nm, y axis) and efficiency (%, x axis) in the margin of the embryo at 5-6 hpf for both $Shp2^{WT}$ and $Shp2^{D61G}$ groups and the impact of ERK activity derived quantified (shadow red arrows). The inversely proportional relationship between AB-FRET R_{DA} and efficiency values in both $Shp2^{WT}$ and $Shp2^{D61G}$ groups distinguishes normal (embryos overexpressing $Shp2^{WT}$, grey dots) and disease (embryos overexpressing $Shp2^{D61G}$, red dots) conditions. For $Shp2^{WT}$ n= 8 and $Shp2^{D61G}$ n = 5.

FRET imaging of *Teen* sensor captures ERK activation changes preceding morphological defects in a RASopathy zebrafish model and phenotypic rescue by MEK inhibitor

Fasano *et al.*,

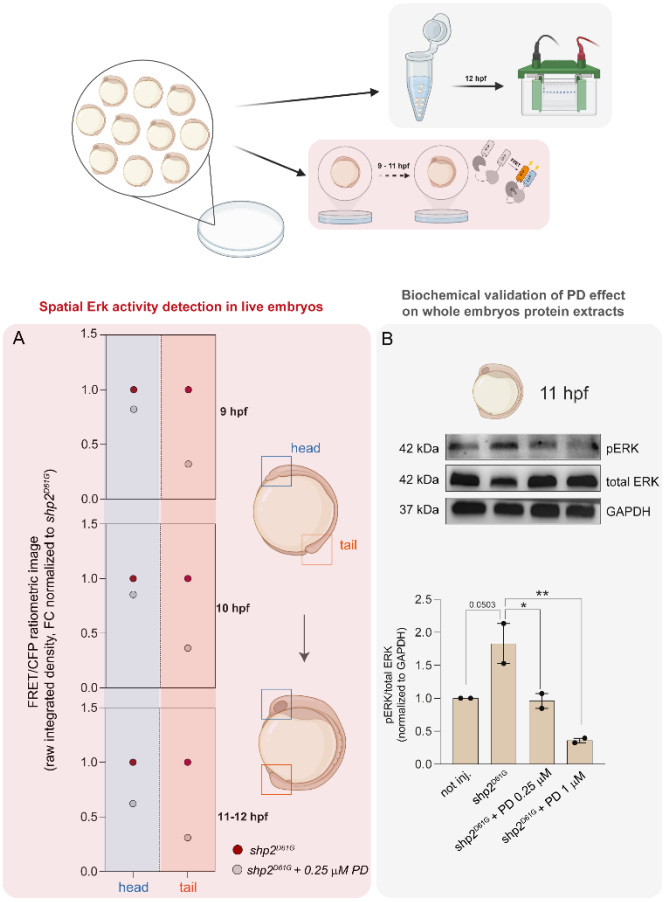

Supplementary Figure 6: Decreased ERK signal in NS embryos (expressing Shp2^{D61G}) treated with low-dose MEK inhibitor as measured by spectral unmixing-FRET during late gastrulae, bud and segmentation stages (9, 10 and 11-12 hpf). Quantification of the ERK signal change in a single live zebrafish embryo expressing Shp2^{D61G} upon treatment with PD 0.25 µM, compared to untreated Shp2^{D61G} and Shp2^{WT} during symptomatic stages in which phenotype rescue can be assessed by measuring axes defects**.** Data for head (blue) and tail (orange) regions are expressed as fold change of the FRET/CFP ratio relative to Shp2^{D61G}.

FRET imaging of *Teen* sensor captures ERK activation changes preceding morphological defects in a RASopathy zebrafish model and phenotypic rescue by MEK inhibitor

Fasano *et al.*,

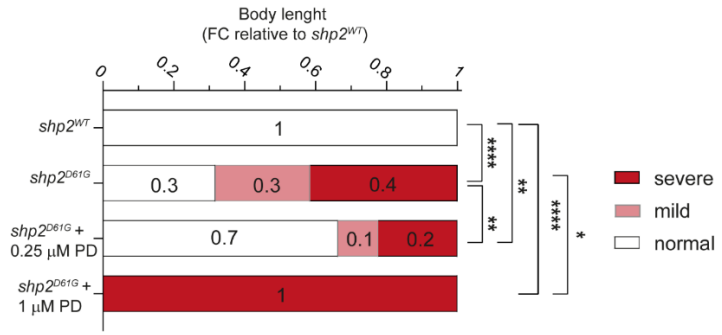

Supplementary Figure 7. Embryo shortening in NS models is rescued by low-dose PD treatment (0.25 μM) but worsened by high doses (1 μM). Percentage of embryos showing normal body length, expressed as FC compared to wild-type embryos (expressing $Shp2^{WT}$) at circa 60 hpf. For $Shp2^{WT}$ n= 15, 23 and 21, 25 for $Shp2^{WT}$, $Shp2^{D61G}$ and $Shp2^{D61G}$ + 0.25 μM and $Shp2^{D61G}$ + 1 μM PD. One-sided Chi-square's test in a 2 × 2 contingency table is used to assess statistical significance ($Shp2^{WT}$ vs. $Shp2^{D61G}$, $Shp2^{WT}$ vs. $Shp2^{D61G}$ + 1 μM PD **** $p < 0.0001$, $Shp2^{D61G}$ vs. $Shp2^{D61G}$ + 0.25 μM PD and $shp2^{WT}$ vs. $Shp2^{D61G}$ + 0.25 μM PD ** $p < 0.01$, $Shp2^{D61G}$ vs. $Shp2^{D61G}$ + 0.25 μM PD * $p < 0.05$).